Pairing Forces Govern Population of Doubly Magic ^{54}Ca from Direct Reactions

F. Browne,[1,*] S. Chen,[2,1,3] P. Doornenbal,[1] A. Obertelli,[4,5,1] K. Ogata,[6,7] Y. Utsuno,[8,9] K. Yoshida,[9] N. L. Achouri,[10] H. Baba,[1] D. Calvet,[5] F. Château,[5] N. Chiga,[1] A. Corsi,[5] M. L. Cortés,[1] A. Delbart,[5] J-M. Gheller,[5] A. Giganon,[5] A. Gillibert,[5] C. Hilaire,[5] T. Isobe,[1] T. Kobayashi,[11] Y. Kubota,[1,8] V. Lapoux,[5] H. N. Liu,[5,12] T. Motobayashi,[1] I. Murray,[13,1] H. Otsu,[1] V. Panin,[1] N. Paul,[5] W. Rodriguez,[14,1,15] H. Sakurai,[1,16] M. Sasano,[1] D. Steppenbeck,[1] L. Stuhl,[8,29] Y. L. Sun,[5] Y. Togano,[17] T. Uesaka,[1] K. Wimmer,[16,1,†] K. Yoneda,[1] O. Aktas,[12] T. Aumann,[4,18] K. Boretzky,[18,1] C. Caesar,[4,18,1] L. X. Chung,[19] F. Flavigny,[13] S. Franchoo,[13] I. Gasparic,[20,4,1] R.-B. Gerst,[21] J. Gibelin,[10] K. I. Hahn,[22,29] M. Holl,[4] J. Kahlbow,[4] D. Kim,[22,29] D. Körper,[18] T. Koiwai,[16] Y. Kondo,[23] P. Koseoglou,[4,18] J. Lee,[2] C. Lehr,[4] B. D. Linh,[19] T. Lokotko,[2] M. MacCormick,[13] K. Miki,[4,24‡] K. Moschner,[21] T. Nakamura,[23] S. Y. Park,[22,29] D. Rossi,[4,18] E. Sahin,[25] F. Schindler,[4] H. Simon,[18] P-A. Söderström,[4] D. Sohler,[26] S. Takeuchi,[23] H. Törnqvist,[4,18] J. Tscheuschner,[4] V. Vaquero,[27] V. Wagner,[4] S. Wang,[28] V. Werner,[4] X. Xu,[2] H. Yamada,[23] D. Yan,[28] Z. Yang,[1] M. Yasuda,[23] and L. Zanetti[4]

[1]*RIKEN Nishina Center, 2-1 Hirosawa, Wako, Saitama 351-0198, Japan*
[2]*Department of Physics, The University of Hong Kong, Pokfulam 999077, Hong Kong*
[3]*State Key Laboratory of Nuclear Physics and Technology, Peking University, Beijing 100871, China*
[4]*Institut für Kernphysik, Technische Universität Darmstadt, 64289 Darmstadt, Germany*
[5]*IRFU, CEA, Université Paris-Saclay, F-91191 Gif-sur-Yvette, France*
[6]*Research Center for Nuclear Physics (RCNP), Osaka University, Ibaraki 567-0047, Japan*
[7]*Department of Physics, Osaka City University, Osaka 558-8585, Japan*
[8]*Center for Nuclear Study, University of Tokyo, RIKEN campus, Wako, Saitama 351-0198, Japan*
[9]*Advanced Science Research Center, Japan Atomic Energy Agency, Tokai, Ibaraki 319-1195, Japan*
[10]*LPC Caen, ENSICAEN, Université de Caen, CNRS/IN2P3, F-14050 Caen, France*
[11]*Department of Physics, Tohoku University, Sendai 980-8578, Japan*
[12]*KTH Royal Institute of Technology, 10691 Stockholm, Sweden*
[13]*IPN Orsay, CNRS and Univiersité Paris-Saclay, F-91406 Orsay Cedex, France*
[14]*Universidad Nacional de Colombia, Sede Bogotá, Facultad de Ciencias, Departmento de Física, Bogotá 111321, Colombia*
[15]*Pontificia Universidad Javeriana, Facultad de Ciencias, Departamento de Física, Bogotá, Colombia*
[16]*Department of Physics, University of Tokyo, 7-3-1 Hongo, Bunkyo, Tokyo 113-0033, Japan*
[17]*Department of Physics, Rikkyo University, 3-34-1 Nishi-Ikebukuro, Toshima, Tokyo 171-8501, Japan*
[18]*GSI Helmholtzzentrum für Schwerionenforschung GmbH, Planckstr. 1, 64291 Darmstadt, Germany*
[19]*Institute for Nuclear Science & Technology, VINATOM, P.O. Box 5T-160, Nghia Do, Hanoi, Vietnam*
[20]*Ruđer Bošković Institute, Bijenička cesta 54,10000 Zagreb, Croatia*
[21]*Institut für Kernphysik, Universität zu Köln, D-50937 Cologne, Germany*
[22]*Ewha Womans University, Seoul 03760, Korea*
[23]*Department of Physics, Tokyo Institute of Technology, 2-12-1 O-Okayama, Meguro, Tokyo 152-8551, Japan*
[24]*National Superconducting Cyclotron Laboratory, Michigan State University, East Lansing, Michigan 48824, USA*
[25]*Department of Physics, University of Oslo, N-0316 Oslo, Norway*
[26]*Atomki, P.O. Box 51, Debrecen H-4001, Hungary*
[27]*Instituto de Estructura de la Materia, CSIC, E-28006 Madrid, Spain*
[28]*Institute of Modern Physics, Chinese Academy of Sciences, Lanzhou 730000, China*
[29]*Institute for Basic Science, Daejeon 34126, Korea*

(Received 11 January 2021; revised 3 March 2021; accepted 29 March 2021; published 23 June 2021)

Direct proton-knockout reactions of ^{55}Sc at ∼220 MeV/nucleon were studied at the RIKEN Radioactive Isotope Beam Factory. Populated states of ^{54}Ca were investigated through γ-ray and invariant-mass spectroscopy. Level energies were calculated from the nuclear shell model employing a phenomenological internucleon interaction. Theoretical cross sections to states were calculated from distorted-wave impulse approximation estimates multiplied by the shell model spectroscopic factors, which describe the wave function overlap of the ^{55}Sc ground state with states in ^{54}Ca. Despite the calculations showing a significant amplitude of excited neutron configurations in the ground-state of ^{55}Sc, valence proton removals populated predominantly the ground state of ^{54}Ca. This counterintuitive result is attributed to pairing effects leading to a dominance of the ground-state spectroscopic factor. Owing to the ubiquity of the pairing interaction, this argument should be generally applicable to direct knockout reactions from odd-even to even-even nuclei.

DOI: 10.1103/PhysRevLett.126.252501

Perhaps the most profound of the interactions within the atomic nucleus is that of *pairing*. It is well described by a strongly attractive contact force between two nucleons (protons and neutrons). Notably, it is why, without exception, even-even nuclei have zero total angular momentum and positive parity ($J^\pi = 0^+$) ground states. Moreover, it is the origin of odd-even staggering of neutron and proton separation energies (S_n and S_p, respectively). Recently, pairing has been shown to have a prominent role in single-nucleon removal cross sections in so-called neutron-rich exotic nuclei which have an excess of neutrons compared to their stable counterparts [1]. In this Letter, a further implication of pairing to direct reactions is demonstrated.

Along with pairing, the interaction of a nucleon's intrinsic (s) and orbital (ℓ) angular momenta has far-reaching consequences. In particular, it is necessary for the theoretical reproduction of the observed nuclear "magic numbers" of stable nuclei, 2, 8, 20, 28, 50, 82… [2,3], which relate to large energy gaps between shells of protons and neutrons. These are termed as *canonical* magic numbers. This reproduction is achieved through the breaking of the energy degeneracy of states with same ℓ and different s orientations, $j_> = \ell + s$ and $j_< = \ell - s$, where $E(j_>) < E(j_<)$. Nuclei with both proton and neutron numbers equalling magic numbers are known as *doubly magic*. A consequence of the pairing interaction, most obvious in doubly magic nuclei, is the existence of excited states based on the promotion of identical nucleon pairs to higher-lying shells, generating 2-particle-2-hole ($2p$-$2h$) states.

The *tensor force* between nucleons is dependent on the vector which connects their spins, and, therefore, does not depend only on their separation distance. A feature of this force is the attraction of unlike nucleons of the same $\ell (= s, p, d, f \ldots)$ and different intrinsic spin orientations, $j_> = \ell + s$ and $j_< = \ell - s$ [4]. It implies an evolution of the energies of the spin-orbit generated shells as a function of nucleon number in exotic nuclei [5,6]. Stable counterparts of neutron-rich nuclei have occupied proton $j_>$ orbits, lowering the corresponding neutron $j_<$ orbital energy. Low occupancy of the proton $j_>$ in the neutron-rich case results in less interaction with the neutron $j_<$ orbital allowing $E(j_<)$ to increase. In ^{54}Ca, this effect, owing to a lack of $\pi(\text{proton})0f_{7/2}$ occupation, allows for a high-lying $\nu(\text{neutron})0f_{5/2}$ orbital which creates the $N(\text{neutron number}) = 34$ magic number, which is not observed in stable nuclei and is designated as a *noncanonical* magic number [7–9]. A direct analog exists in ^{24}O where an unoccupied $\pi 0d_{5/2}$ orbital allows a large gap between $\nu 0d_{3/2}$ and $\nu 1s_{1/2}$ to form. Substantial compared even to the nearby ^{27}Ne [10], this leads to the noncanonical $N = 16$ magic number in the O isotopes [11,12].

There is some recent evidence that the removal of the valence proton from the $\pi 0d_{5/2}$ orbital in ^{25}F leads to ~60% population of excited states of ^{24}O [13]. This implies a large overlap of the ground-state wave function of ^{25}F with excited-state wave functions of ^{24}O. The magnitude of this overlap is known as the *spectroscopic factor*. The explanation for the large population of excited states in Ref. [13] was the induced configuration mixing of the ^{24}O core neutron states by the lowering of the $\nu 0d_{3/2}$ energy to emulate the effect of a strengthened tensor force with the $\pi 0d_{5/2}$ proton. However, from the point of view of the pairing interaction, the spectroscopic factor to the ground-state would be expected to be large. This can be illustrated in a two-level model of $0p$-$0h$ (ground state) and $2p$-$2h$ neutron states for ^{25}F and ^{24}O. The spectroscopic factor to the ground state of ^{24}O following a $\pi 0d_{3/2}$ proton removal is dependent on the product of amplitudes of the $2p$-$2h$ states in the wave functions of ^{25}F and ^{24}O. This product is positive owing to the definite signs of the off-diagonal two-body matrix elements of the pairing interaction [14].

Whether the population patterns from direct $^{55}\text{Sc}(p, 2p)$ proton removal reactions adhere to the pairing interaction expectation or reflect excited neutron configurations as a consequence of the tensor force is addressed in this Letter. As with ^{25}F, ^{55}Sc has a noncanonical doubly magic core that results from the absence of the tensor force attraction and a single proton in the orbital that acts to lower the valence neutron energies. In the present work and Ref. [13], projectiles were produced under the same conditions and the same reaction is employed at energies of ~220 and 270 MeV/nucleon, respectively.

The first study of ^{54}Ca populated through direct single-nucleon knockout reactions is presented. Cross sections to ground and excited states, known as exclusive cross sections, have been measured as well as ℓ values of removed nucleons that populated them. Only through application of invariant-mass spectroscopy to the heaviest exotic nucleus to date were such measurements possible for the unbound states. Comparisons of the measurements were made to distorted-wave impulse approximation (DWIA) [15,16] and conventional shell model calculations, i.e., relying on direct diagonalization of the Hamiltonian, the latter employing the GXPF1Br internucleon interaction [7] in the full sd-pf-gds model space, which lies below the magic number 82. From the comparisons, ℓ values of removed nucleons and tentative J^π assignments to excited states of ^{54}Ca were determined. The results show predominant ground- and excited-state population of ^{54}Ca through valence and core proton removals, respectively.

Experimental investigations were conducted at the Radioactive Isotope Beam Factory, operated by the RIKEN Nishina Center and the Center for Nuclear Study, University of Tokyo. A 240 pnA beam of $^{70}\text{Zn}^{30+}$ was accelerated to 345 MeV/nucleon and secondary beams of isotopes were produced from its fragmentation on a 10-mm-thick ^{9}Be target situated at the entrance of BigRIPS [17], a two-stage fragment separator. Specific constituents of the secondary beam cocktail were selected

and separated up until the 3rd focal plane of BigRIPS by their magnetic rigidity ($B\rho$) through two dipole magnets and energy loss (ΔE) through an Al wedge-shaped degrader situated between the dipole magnets. The time of flight (TOF), $B\rho$, and ΔE were recorded for each ion between the 3rd and 7th focal planes. These measurements were combined to provide unambiguous particle identification (PID) of the ions' mass-to-charge ratio and atomic number [18], shown in Fig. 1(a). Following identification, the secondary beams were transported to the MINOS device [19], a 151(1)-mm-long liquid hydrogen (LH_2) target surrounded by a time projection chamber (TPC) situated at the focal plane designated "F13," which is ~40 m downstream of the 7th focal plane. Surrounding MINOS was the DALI2$^+$ array of 226 NaI(Tl) crystals [20,21] for the high-efficiency detection (~23% for a 2 MeV γ ray emitted at $\beta_{\rm ion} \approx 0.6$) of γ rays emitted by excited states populated by secondary reactions. Downstream of MINOS, reaction residues were identified, as shown in Fig. 1(b), with the SAMURAI spectrometer by their $B\rho$ through a single dipole magnet, TOF from the target to a hodoscope, and energy loss in the hodoscope [22]. Reaction vertices in the LH_2 target were identified with a precision of ~2 mm (σ) by tracking incoming fragments with beam-line detectors and tracking protons ejected from the target with the surrounding TPC [23]. Fragment velocities at the reaction vertex were reconstructed using the vertex position and velocity measured in SAMURAI. Beam-velocity neutron detection was realized with NEBULA [22,24], comprising two assemblies of 60 vertically aligned $12 \times 12 \times 180$ cm^3 detectors arranged in a 2×30 configuration, and NeuLAND [25], one assembly of 400 $5 \times 5 \times 250$ cm^3 detectors arranged in alternating vertically and horizontally aligned planes of 50 detectors. The center of NeuLAND was 11.8 m from the center of the LH_2 target, and the two NEBULA assemblies were at 14.4 and 15.3 m. Neutron energies were calculated from their velocities which were derived from their TOFs and flight paths.

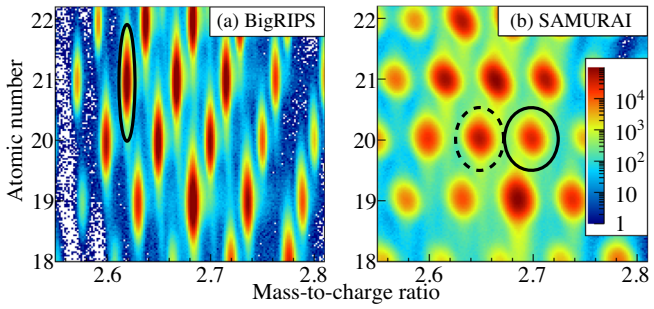

FIG. 1. Identified ions in front of (a) and behind (b) the reaction target. In (a), the ellipse indicates the software gate placed on ^{55}Sc. In (b), gates applied to select ^{53}Ca and ^{54}Ca are shown as dashed and solid ellipses, respectively. The scale is counts per bin and applies to (a) and (b).

Doppler-corrected γ-ray spectra following the ^{55}Sc$(p,2p)$ reaction, Fig. 2(a), show γ-ray peaks at 445(16), 1210(30), 1661(17), and 2021(17) keV, consistent with Ref. [7]. A double-exponential background models the shallow background at high energy and steep background below ~500 keV. Coincidences between the 2021-keV transition and all others were observed, shown in the inset of Fig. 2(a), with intensities which imply the level scheme shown in Fig. 2(a). Also apparent in the coincidence spectrum is an excess of counts at ~560 keV, with a corresponding excess in the singles spectrum. Assuming this takes the form of a γ-ray transition, a fitted value of 561(19) keV is obtained with a 0.04(2) mb cross section. With a significance of just over 1σ, it is not considered in the calculation of other partial cross sections. The parallel momentum distributions (PMDs) of the reaction products in coincidence with their populated state provides information on the ℓ-value of the removed nucleon. PMDs of ^{54}Ca nuclei in the ground, Fig. 2(c), and (3^-), Fig. 2(d), states were measured with a resolution of ~34 MeV/c (σ) which was inferred from unreacted ^{55}Sc nuclei [26]. The ground-state PMD is consistent with the removal of an f-wave proton and the (3^-) PMD has χ^2/degree of freedom for the d and f curves of 0.56 and 0.64, respectively, slightly favoring the removal from a d orbital. The f-like PMD of the ground-state population supports previous evidence for a $J^\pi = 7/2^-$ ^{55}Sc ground state [27] as it almost certainly reflects a valence $\pi 0f_{7/2}$ orbital. Since the 2_1^+ state population is dominated by feeding from the (3^-) state, its PMD only reflects the (3_1^-) structure, it can be found with the inclusive PMD in Ref. [26]. From these observations and those in Ref. [7], a 3_1^- state with a $\pi 0f_{7/2}^1 0d_{3/2}^{-1}$ configuration is suggested for the 3680(20) keV level.

Decays of unbound states of ^{54}Ca, first inferred through inelastic scattering [9], are shown in the relative energy ($E_{\rm rel}$) spectrum of ^{53}Ca and respective emitted neutrons in Fig. 2(b). $E_{\rm rel}$ spectra in coincidence with individual states of ^{53}Ca, termed exclusive spectra, were used to isolate overlapping peaks and construct the decay scheme shown in Fig. 2(b) [26]. Peaks in the exclusive spectra were fitted with Breit-Wigner distributions [29] folded with experimental responses of the NeuLAND + NEBULA array and beam-line detectors, further details are given in Ref. [26]. A low-amplitude background with a shape generated from event-mixing [30,31] is consistent with a high-statistics study performed with a similar experimental set-up [32]. Transitions strengths at 0.102(21), 0.546(58), and 2.92(12) MeV were identified in coincidence with the ^{53}Ca ground state, at 0.1013(54), 0.583(13), 1.224(74), and 1.955(45) MeV with the 1738-keV state, and at 0.385(13), 0.672(21), and 1.454(33) MeV with the 2220-keV state. The low uncertainty associated with the 0.1013-MeV strength is attributed to the narrow width and high statistics of the peak in the exclusive spectrum [26].

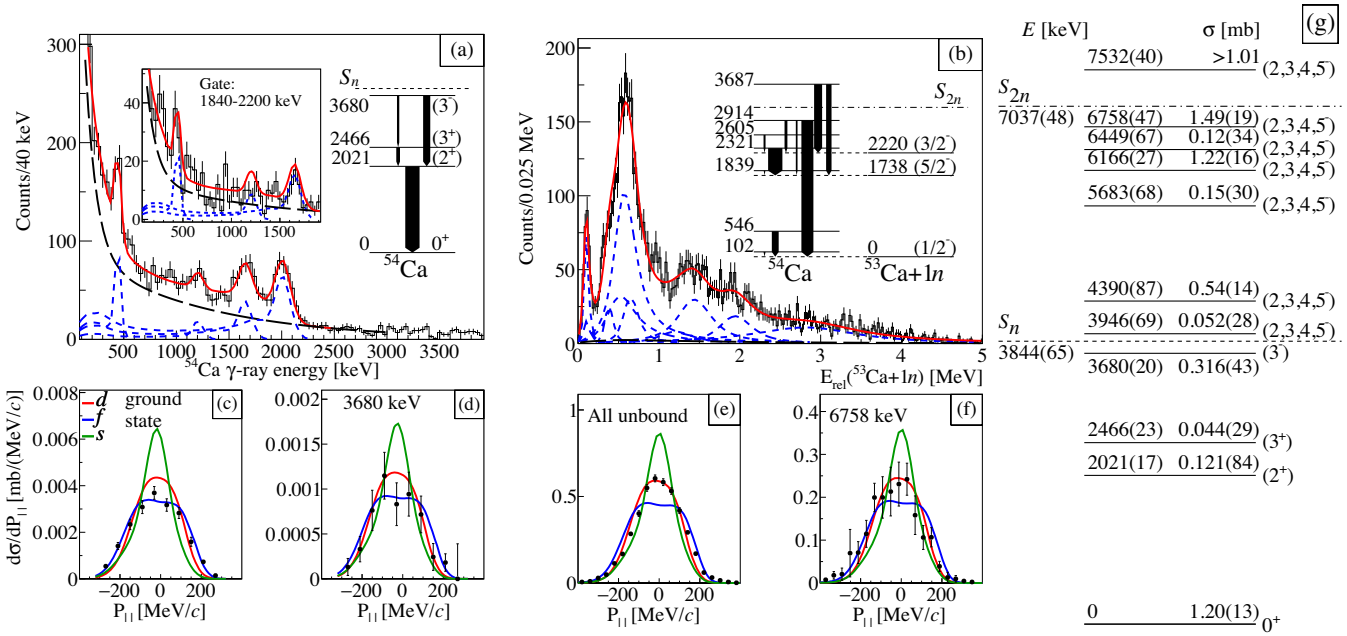

FIG. 2. (a) Doppler-corrected γ-ray spectrum of the $^{55}\mathrm{Sc}(p,2p)$ reaction populating bound states. The total fit function (red line) comprises simulated response functions of DALI2^{+} (blue short-dashed lines) and a double-exponential background (black long-dashed line). The inset spectrum is that in coincidence with the 2021-keV transition, where the blue dashed lines are intensity-fixed responses assuming the shown level scheme. Arrow widths on the level scheme represent relative γ-ray intensities. (b) Relative energy spectrum of $^{55}\mathrm{Sc}(p,2p)^{54}\mathrm{Ca} \rightarrow {}^{53}\mathrm{Ca} + 1n$. The total fit function (red line) is the sum of the simulated responses of NeuLAND + NEBULA and beam-line detectors (blue short-dashed lines), and a nonresonant background (black long-dashed line). Inset is the decay scheme to ^{53}Ca, level energies are with respect to the ^{53}Ca ground-state energy and arrow widths are relative decay strengths. (c)–(f) PMDs of residual ^{54}Ca (c),(d) and $^{53}\mathrm{Ca} + 1n$ (e),(f) following $^{55}\mathrm{Sc}(p,2p)$ reactions in coincidence with various states. "All unbound" infers the inclusive PMD for unbound states, otherwise labels of (c)–(f) correspond to (g), which shows the energies, cross sections, and J^{π} assignments of observed states. Data points in (c)–(f) are observed and solid curves are predicted by the DWIA for the d-, f-, and s-wave proton removals normalized to experimental cross sections. Where appropriate, S_n and S_{2n} [28] values are indicated.

Summing the decay energies with their coincident ^{53}Ca state energies suggests that the 2.92-, 1.224-, and 0.672-MeV decays depopulate a common state, as do the 1.955- and 1.454-MeV decays, leading to the decay scheme shown in Fig. 2(b). The strengths and their cross sections are summarized in Fig. 2(g), where the given energy is the centroid of the peak that best describes the observed distribution, and does not necessarily reflect the energy of a single state. An exclusive PMD was extracted for the level strength at 6758 keV, as shown in Fig. 2(f), owing to its ~3-MeV decay being isolated in the E_{rel} spectrum of Fig. 2(b), and conforms to a d-wave proton removal. Other exclusive cross sections do not provide conclusive results. The inclusive PMD for the full E_{rel} strength, Fig. 2(e), is consistent with a d-wave proton removal. Assuming a $\pi 0d_{3/2}$ proton removal and a $7/2^{-}$ ^{55}Sc ground state, as suggested by Fig. 2(c), gives possible $J^{\pi} = 2, 3, 4, 5^{-}$ for the unbound states. Therefore, most observed excited states shown in Fig. 2(g) are likely of $\pi 0f_{7/2}^{1} 0d_{3/2}^{-1}$ structure. The relative energy spectrum of $^{55}\mathrm{Sc}(p,2p)^{54}\mathrm{Ca}^{*} \rightarrow {}^{52}\mathrm{Ca} + 2\,n$ has too few statistics for interpretation.

Figure 2(g) and the upper panel of Fig. 3 summarize measured level energies and population cross sections from this work. Theoretical cross sections and energies are displayed in the lower panel of Fig. 3. Energies were calculated from the shell model using the GXPF1Br interaction in the full sd-pf-gds model space, including both $0g_{7/2}$ and $0g_{9/2}$ orbitals. Cross sections are those of the DWIA single-particle values scaled with spectroscopic factors from the same calculation as used for the energies [26]. Measured cross sections of the 0_1^{+}, 1.20(13) mb, and (2_1^{+}), 0.121(84) mb, states are reproduced by the calculated ones of 1.65 and 0.086 mb, respectively. Moreover, the measured (2_1^{+}) energy is in agreement with theory. Some population of the 0_2^{+} state is predicted with a cross section consistent with that of the low-significance 561-keV γ-ray candidate, not shown in Fig. 3. To a very good approximation, the predicted 3_1^{+} state at 2.99 MeV has zero cross section, consistent with observation of the (3_1^{+}) state at the lower 2.47 MeV. The predicted 3_1^{-} state is unbound, contrary to observation, however, the measured cross section, 0.316(43) mb, agrees well with the predicted 0.35 mb. It is noteworthy that similar contributions to the

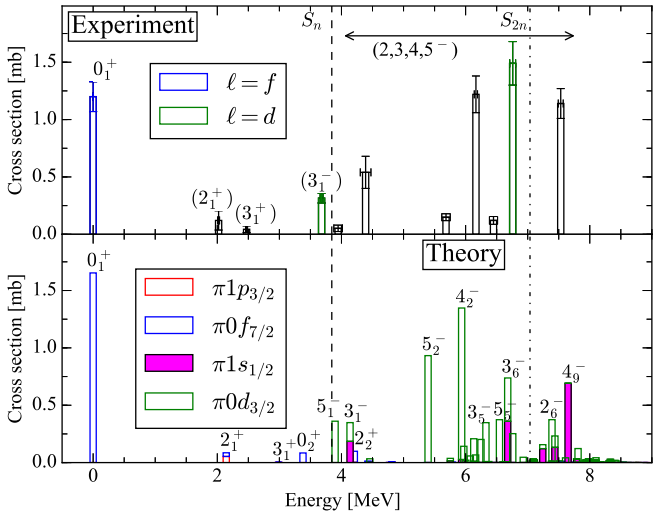

FIG. 3. (Top panel) Below S_n, the measured cross sections to states from γ-ray spectroscopy are shown. Above S_n, the population cross sections of the unbound strengths from invariant mass spectroscopy are shown at the energy centroids of fitted values and likely represent contributions from several states. States with conclusive PMDs are colored accordingly to the ℓ value of their removed nucleon, otherwise are black. (Bottom panel) Theoretical predictions of state energies and their population cross sections are shown. Contributions to cross sections from proton removals from the different orbitals are indicated. Unlabeled levels have $J^\pi = 2, 3, 4, 5^-$.

3_1^- state from the $\pi 1s_{1/2}$, 0.19 mb, and $\pi 0d_{3/2}$, 0.16 mb, orbitals are predicted. The state's experimental PMD shown in Fig. 2(d) does not reflect such a contribution from the $\pi 1s_{1/2}$ orbital. The inclusive cross section to bound states was measured to be 1.69(3) mb, close to the predicted 1.83 mb, and inline with observed quenching from similar reactions populating N and O isotopes [33,34]. Above S_n, it is stressed that while the cross sections are indicated at the level energies shown in Fig. 2(g) and the top panel of Fig. 3, they are likely distributed across many unresolvable states, however, so long as the origin of the excitation strength is accounted for, this does not change the conclusions of this work. In the following discussion, the excitation strengths are identified to determine any presence of excited-state population from valence proton removal. The location of level strengths are in broad agreement with prediction. Between S_n and S_{2n} a total level strength of 3.57(30) mb is observed, which is 67(6)% of the predicted 5.30 mb, after subtracting the 3_1^- contribution, in agreement with the anticipated quenching of the single-particle strengths [33,34]. This exhaustion of strength leaves no observed strength that can be attributed to the removal from the valence $\pi 0f_{7/2}$ orbital. Beyond S_{2n}, within the experimentally sensitive range, a total level population cross section of 2.12 mb is predicted, compared to a lower limit of > 1.01 mb deduced from a 1.14(13) mb strength in the $1n$ channel. For the strengths beyond S_{2n}, direct comparison to theory is difficult owing to the lack of sensitivity to the $2n$ decay channel. Proton removal from $\pi 0d_{3/2}$ dominates the excited states, reflected by the inclusive PMD. Whilst a strong population of the 3_6^- and 4_9^- states following $\pi 1s_{1/2}$ proton removal are predicted, it is not observed clearly in any PMD, possibly due to the influence of states populated by $\pi 0d_{3/2}$ proton removal. Since these are not valence-proton removals, their presence, or not in the data has no bearing on the following discussion.

Negligible population of excited states of ^{54}Ca originates from the proton removal from $\pi 0f_{7/2}$ in ^{55}Sc. All excited states are consistent with population from core-proton removals, predominantly from $\pi 0d_{3/2}$, and potentially $\pi 1s_{1/2}$. These findings are contrary to the analogous case of ^{25}F$(p, 2p)$ [13], in which valence proton removals preferentially populated excited states of ^{24}O.

The shell model calculations result in $0p$-$0h$ (closed $N = 34$ shell) contributions of the ^{55}Sc and ^{54}Ca ground-state wave functions as 64.2% and 89.4%, respectively. The remainder of the contributions are dominated by $2p$-$2h$ configurations. Despite this erosion of the $N = 34$ closure in ^{55}Sc, which is supported by experiment [35,36], the spectroscopic factors (C^2S) show removal from $\pi 0f_{7/2}$ mostly populates the ground-state of ^{54}Ca, as observed experimentally. This can be understood through a simple two-level system of both ^{55}Sc and ^{54}Ca. Assuming each have wave functions that only have contributions from $0p$-$0h$ (ϕ_{0p0h}) and $2p$-$2h$ (ϕ_{2p2h}) configurations,

$$\Psi(^{55}\mathrm{Sc}) = \alpha_{0p0h}\phi_{0p0h}(^{55}\mathrm{Sc}) + \alpha_{2p2h}\phi_{2p2h}(^{55}\mathrm{Sc}),$$
$$\Psi(^{54}\mathrm{Ca}) = \beta_{0p0h}\phi_{0p0h}(^{54}\mathrm{Ca}) + \beta_{2p2h}\phi_{2p2h}(^{54}\mathrm{Ca}),$$

where α and β are real numbers satisfying $\alpha_{0p0h}^2 + \alpha_{2p2h}^2 = 1$ and $\beta_{0p0h}^2 + \beta_{2p2h}^2 = 1$. With vanishing overlaps of ϕ_{0p0h} and ϕ_{2p2h}, the spectroscopic factor to the ground state of ^{54}Ca can be expressed as

$$C^2S_{\mathrm{g.s.}} = (\alpha_{0p0h}\beta_{0p0h} + \alpha_{2p2h}\beta_{2p2h})^2. \quad (1)$$

Since pairing forces have a definite sign in their off-diagonal two-body matrix elements, the amplitudes α_{2p2h} and β_{2p2h} take on the same sign [14]. Therefore, $\alpha_{2p2h}\beta_{2p2h} > 0$ leading to a large $C^2S_{\mathrm{g.s.}}$ following the removal of a valence proton. From the two-state model discussed above, $\alpha_{0p0h} = \sqrt{0.642}$, $\beta_{0p0h} = \sqrt{0.894}$, $\alpha_{2p2h} = \sqrt{1 - \alpha_{0p0h}^2}$, and $\beta_{2p2h} = \sqrt{1 - \beta_{0p0h}^2}$, Eq. (1) yields $C^2S_{\mathrm{g.s.}} = 0.907$, and from the full calculation, including all other contributions, $C^2S_{\mathrm{g.s.}} = 0.828$ for the proton removal from $\pi 0f_{7/2}$. For the singly occupied $\pi 0f_{7/2}$ orbital, $\sum C^2S \approx 1$, leaving little remaining

spectroscopic strength available to excited states. Therefore, despite the configuration mixing of the ^{54}Ca core of ^{55}Sc due to the tensor force, conditions resulting from the pairing force lead to dominant ground-state population following valence proton removal.

In conclusion, the ground and excited states of the noncanonical doubly magic ^{54}Ca have been populated through direct proton-knockout reactions on a LH_2 target from ^{55}Sc. Orbital angular momenta of removed protons were inferred through PMDs of reaction residues. An additional bound state was placed in the level scheme of ^{54}Ca [7], and level strengths charted to beyond the S_n threshold through γ-ray and invariant-mass spectroscopy, the latter being for the first time applied to such a heavy neutron-rich system. All observed excited states populated through the $^{55}\mathrm{Sc}(p,2p)$, reaction were attributed to removal of protons from the ^{54}Ca core. Valence-proton removals populated predominantly the ground-state of ^{54}Ca despite significant neutron-excitation amplitudes in the ground-state configuration of ^{55}Sc. The reasoning behind this was the constructive effects from the pairing interaction on the ground-state spectroscopic factor, exhausting the strength available to excited states. Considering the ubiquity of the pairing interaction, it is interesting this effect is seemingly overridden by tensor forces in the $^{25}\mathrm{F}(p,2p)$ case [13]. It is noteworthy that the experiment carried out in Ref. [13] did not have beam-velocity neutron-detection capability. An experiment similar to the one reported here would enable the population of individual unbound states of ^{24}O to be quantitatively studied, leading to a more robust comparison to the predicted spectroscopic factors. With such information, the interplay of the tensor force and pairing interactions in direct reactions could be consolidated.

Our gratitude is extended to the RIKEN Nishina Center accelerator staff for the stable and high-intensity transport of the Zn primary beam, and the BigRIPS team for their preparation of the magnetic settings of the secondary beam. F. B. is supported by the RIKEN Special Postdoctoral Researcher Program. S. C. acknowledges support from the IPA program at the RIKEN Nishina Center. K. O. and K. Y. acknowledge the support from Grants-in-Aid of the Japan Society for the Promotion of Science under Grants No. JP16K05352. This work was supported by JSPS KAKENHI Grants No. JP16H02179 and No. JP18H05404, the Deutsche Forschungsgemeinschaft (DFG, German Research Foundation) under Grant No. BL 1513/1-1 HGS-HIRe and Project-ID 279384907-SFB 1245 and the GSI-TU Darmstadt cooperation agreement, the BMBF (Grant No. 05P19RDFN1), Swedish Research Council under Grants No. 621-2014-5558 and No. 2019-04880. L. X. C. and B. D. L. are supported by the Vietnam MOST via the Physics Development Program Grant No. ĐTĐLCN.25/18. D. So. was supported by the European Regional Development Fund Contract No. GINOP-2.3.3-15-2016-00034 and the National Research, Development and Innovation Fund of Hungary via Project No. K128947. L. S, K. I. H., D. K., and S. Y. P. acknowledge the support from the IBS grant funded by the Korea government (No. IBS-R031-D1).

*frank@ribf.riken.jp
†Present address: Instituto de Estructura de la Materia, CSIC, E-28006 Madrid, Spain.
‡Present address: Department of Physics, Tohoku University, 6-3 Aramaki-Aoba, Aoba, Sendai 980-8578, Japan.

[1] N. Paul *et al.*, Phys. Rev. Lett. **122**, 162503 (2019).
[2] M. G. Mayer, Phys. Rev. **75**, 1969 (1949).
[3] O. Haxel, J. H. D. Jensen, and H. E. Suess, Phys. Rev. **75**, 1766 (1949).
[4] T. Otsuka, T. Suzuki, R. Fujimoto, H. Grawe, and Y. Akaishi, Phys. Rev. Lett. **95**, 232502 (2005).
[5] T. Otsuka, R. Fujimoto, Y. Utsuno, B. A. Brown, M. Honma, and T. Mizusaki, Phys. Rev. Lett. **87**, 082502 (2001).
[6] T. Otsuka, A. Gade, O. Sorlin, T. Suzuki, and Y. Utsuno, Rev. Mod. Phys. **92**, 015002 (2020).
[7] D. Steppenbeck *et al.*, Nature (London) **502**, 207 (2013).
[8] S. Michimasa *et al.*, Phys. Rev. Lett. **121**, 022506 (2018).
[9] S. Chen *et al.*, Phys. Rev. Lett. **123**, 142501 (2019).
[10] A. Obertelli *et al.*, Phys. Lett. B **633**, 33 (2006).
[11] C. R. Hoffman *et al.*, Phys. Rev. Lett. **100**, 152502 (2008).
[12] R. Kanungo *et al.*, Phys. Rev. Lett. **102**, 152501 (2009).
[13] T. L. Tang *et al.*, Phys. Rev. Lett. **124**, 212502 (2020).
[14] S. Yoshida, Nucl. Phys. **33**, 685 (1962).
[15] K. Ogata, K. Yoshida, and K. Minomo, Phys. Rev. C **92**, 034616 (2015).
[16] T. Wakasa, K. Ogata, and T. Noro, Prog. Part. Nucl. Phys. **96**, 32 (2017).
[17] T. Kubo *et al.*, Prog. Theor. Exp. Phys. **2012**, 03C003 (2012).
[18] N. Fukuda, T. Kubo, T. Ohnishi, N. Inabe, H. Takeda, D. Kameda, and H. Suzuki, Nucl. Instrum. Methods Phys. Res., Sect. B **317**, 323 (2013).
[19] A. Obertelli *et al.*, Eur. Phys. J. A **50**, 8 (2014).
[20] S. Takeuchi, T. Motobayashi, Y. Togano, M. Matsushita, N. Aoi, K. Demichi, H. Hasegawa, and H. Murakami, Nucl. Instrum. Methods Phys. Res., Sect. A **763**, 596 (2014).
[21] I. Murray *et al.*, RIKEN Accel. Prog. Rep. **51**, 158 (2018), https://www.nishina.riken.jp/researcher/APR/APR051/pdf/158.pdf.
[22] T. Kobayashi *et al.*, Nucl. Instrum. Methods Phys. Res., Sect. B **317**, 294 (2013).
[23] C. Santamaria *et al.*, Nucl. Instrum. Methods Phys. Res., Sect. A **905**, 138 (2018).
[24] T. Nakamura and Y. Kondo, Nucl. Instrum. Methods Phys. Res., Sect. B **376**, 156 (2016).
[25] T. Aumann, Technical report for the design, construction and commissioning of NeuLAND: The high-resolution neutron time-of-flight spectrometer for R3B, Technical Report, FAIR, 2011, https://edms.cern.ch/ui/file/1865739/2/TDR_R3B_NeuLAND_public.pdf.

[26] See Supplemental Material at http://link.aps.org/supplemental/10.1103/PhysRevLett.126.252501 for inclusive and (2_1^+) PMDs, exclusive E_{rel} spectra and associated fit details, full results of theoretical calculations.
[27] H. L. Crawford *et al.*, Phys. Rev. C **82**, 014311 (2010).
[28] F. Wienholtz *et al.*, Nature (London) **498**, 346 (2013).
[29] A. M. Lane and R. G. Thomas, Rev. Mod. Phys. **30**, 257 (1958).
[30] G. Randisi *et al.*, Phys. Rev. C **89**, 034320 (2014).
[31] S. Leblond *et al.*, Phys. Rev. Lett. **121**, 262502 (2018).
[32] A. Revel *et al.* (SAMURAI21 Collaboration), Phys. Rev. Lett. **124**, 152502 (2020).
[33] L. Atar *et al.* (R^3B Collaboration), Phys. Rev. Lett. **120**, 052501 (2018).
[34] M. Gómez-Ramos and A. Moro, Phys. Lett. B **785**, 511 (2018).
[35] D. Steppenbeck *et al.*, Phys. Rev. C **96**, 064310 (2017).
[36] E. Leistenschneider *et al.* (The LEBIT and the TITAN Collaborations), Phys. Rev. Lett. **126**, 042501 (2021).